Comitato Nazionale Energia Nucleare

IT7900038

NEUTRON FLUX SHAPE EFFECTS IN LARGE FAST REACTOR SAFETY CALCULATIONS

A. GALATI, P. LOIZZO, A. MUSCO

Paper for ENS/ANS Topical meeting on Nuclear Power Reactor Safety.
Brussels, Belgium, October 16-19, 1978

CNEN -

RT/FI(78)20

Comitato Nazionale Energia Nucleare

NEUTRON FLUX SHAPE EFFECTS IN LARGE FAST REACTOR SAFETY CALCULATIONS

A. GALATI, P. LOIZZO, A. MUSCO

Paper for ENS/ANS Topical meeting on Nuclear Power Reactor Safety.
Brussels, Belgium, October 16-19, 1978

RT/FI(78)20

Testo pervenuto nel novembre 1978

Riprodotto in offset presso il Laboratorio Tecnografico della Direzione Centrale Relazioni Esterne del CNEN - Viale Regina Margherita 125, Roma

C.N.E.N. - CSN CASACCIA - ROMA (ITALY)

A. Galati, P. Loizzo, A. Musco

NEUTRON FLUX SHAPE EFFECTS IN LARGE FAST REACTOR SAFETY CALCULATIONS

INTRODUCTION

The use of point kinetics model in fast reactor safety calculations is traditionally based on the outstanding virtue that it yields very inexpensive neutronic solutions. However, it implies that the neutron flux shape, i.e. the neutron distribution in space and energy, can be taken as time-independent, so that only the flux level varies with time. This hypothesis can be reasonably adopted for experimental and/or small reactors, where the tight coupling limits the spatial flux deformation to the immediate surrounding of any perturbation. However, the large fast reactor plants are less tightly coupled. The purpose of the present work is precisely to define the reliability of point kinetics methods in large plants safety calculations. To this aim the multigroup two-dimensional (r-z geometry) core dynamics code NADYP-2 was used. Doppler effect, sodium density reactivity and some deformation effects were the main contributors to feedback reactivity. The introduction in the code of a point kinetics module allowed comparisons between two and zero-dimensional calculations to be performed. In the latter the spatial distribution of power was proportional to the stationary one and the energy distribution of neutron flux was necessarily constant in time. Both the 2D and 0D calculations were performed by using spatial dependent thermohydraulics modules; however they were stopped at the starting of the fuel boiling, since the NADYP-2 lacks the dispersion module.

The main features of the reference reactor were the following ones:

- thermal power: 3000 Mw;

- core volume: 10400 lt;
- core height: 1 m;
- two core enrichments, with the ratio (outer core volume)/(inner core volume) $\simeq$ 0.85;
- two control rod banks, the former within the inner core, the latter at the boundary between the two cores.

For computational purposes, the reactor map was divided into ten shells: four for the inner core, two for the outer one, two for the control regions, one for the radial blanket, one for the radial reflector. In the thermohydraulics calculations each shell was described by a single pin model including temperature-dependent physical properties. The metastatic method was employed in the neutron kinetics calculations: in the 2D-cases, five energy groups of prompt neutrons were considered; the delayed neutron groups were always six with β = 0.00347, so that 1 \$ = 347 pcm.

Three classes of accidents were considered:

1) TOP-REX - Space-uniform, time linear changes on the number of fission neutrons generated "external reactivity" which started the accident. This transient starting model represents the minimum deviation from the traditional logic of point kinetics methods in power transients, but it does not simulate any physical process. Three principal TOP-REX cases were studied, corresponding to external reactivity ramps of 40 \$/sec (Case 1), 0.5 \$/sec (Case 2) and 10 \$/sec (Case 3) respectively. In the first one, the role of the steady state flux distribution in the shape effect was also analyzed by changing the control rods position.
2) TOP-BAR - Only one transient of this type was studied (Case 4). It was started by the uniform motion of the six control rods of the inner bank, so that the cylindrical simmetry was preserved. The extraction rate was selected in such a manner that a mean rod reactivity ramp of about 0.5 \$/sec was generated: significant comparisons with Case 2 were made possible by this choice.

3) LOF - These transients were started by hyperbolic reduction of sodium inlet flow-rate to simulate pump failure. Two cases were studied, corresponding to different mechanical inertia of the cooling system: the initial flow halving-time was 50 secs in the LOF-RIF case and 16.7 secs in the LOF-RAP case respectively. The LOF-RIF case in the 0D version was studied also by accounting for the local interference of the sodium voids on the Doppler effect, so that the main spectral component of the shape effect was elided. A reference static, 27-neutron-energy-group calculation showed that the sodium voiding reduces the Doppler effect by a factor 0.61: the spectral corrected 0D version (0DC) contains this factor. The same calculation in our 5-group model gave about the same result, so that no corrections were needed.

RESULTS

The power histories during the TOP-REX and TOP-BAR transients are shown in the first page of the annexed plots. Due to the different behaviours, it is proper to separate the analysis into two parts:

1) TOP-REX - It is evident from plots that the maximum difference between 2D and 0D-calculated powers does not exceed 10%; the same statement holds for the reactivity histories, so that the shape effect is negligible in these cases. Due to the short duration of the transients (when compared with the thermal time-constants of oxide fuel)

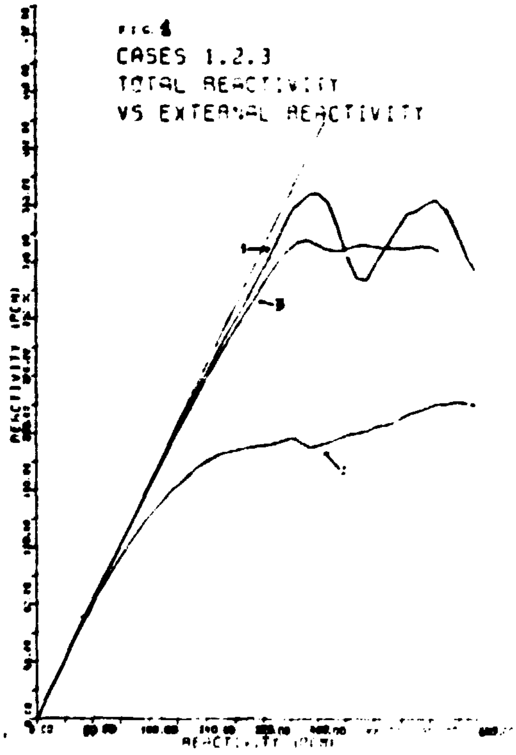

the sodium temperature changes are too little to produce significant reactivity effects: so, only the Doppler feedback is efficient. Its role is evidenced in Fig. 1, where the total reactivity is represented as a function of the external reactivity: due to the different scales, the straight line coincides with the axes bisector. During the "first phase" of the transients, the Doppler effect is negligible too: so, the only possible source of shape effect is represented by the kinetics absorptions, which are defined by the terms $v_k^{-1}\,\partial\phi_k/\partial t$, $k = 1, 2, \ldots .,$ in the diffusion equations. It is well known that these terms are negligible in subprompt-critical excursions. Consequently, the uniform change of the number of fission neutrons will not produce changes in the flux distribution. In the "second phase", the effectiveness of the Doppler effect tends to depress the epithermal flux more in high-power zones than in low-power ones, but this spatial effect is very small, because the epithermal flux is flat and is a small percentage of the total flux.

Shell Time (secs)	1	3	4	5	7	8
0.0	9.9	19.9	29.5	33.6	41.9	30.0
1.0	16.6	29.6	42.5	48.2	59.8	42.8
1.4	23.3	39.5	55.8	62.9	77.8	55.5
2.2	46.1	71.7	97.7	108.6	133.3	94.9
2.9	78.2	113.1	148.0	163.4	199.1	141.5
3.59	171.0	230.0	292.1	315.1	380.5	269.9

Tab. 1

Power/rod (kw) in the core shells (Case 4)

Another calculation was performed to verify the role of the Doppler effect when the flux peaks are emphasized. To this aim, both control rod banks were inserted 40 cm in the core, while in Cases 1, 2, 3 they were considered out of the core. Only the fast transient was repeated. The changes in the power and reactivity histories were very small: even smaller was the change in the shape effect.

2) TOP-BAR - In this case, the shape effect is very large: the ratio 2D-power/0D-power increases with time up to a value of 4.34 at the end of the transient. It is to be noted that the control rod reactivity is generally overvalued in the r-z geometry. However, on the basis of proper static calculations,we have concluded that this effect does not exceed 17% of the involved reactivity, so that it appears unessential to the optics of this work.

The large spatial flux deformations are the main contributors to the 0D-error. The axial neutron flux distribution is strongly modified by the control rods motion, particularly in the inner core, where the power peak shifts 20 cm up.The radial distribution of the power density at different times is reported in Table 1 to quantify the increasing relative importance of the inner core (shells 1 and 3), particularly of shell 1. The 0D calculation does not account for these changes in coupling, so that the reactivity is undervalued. The contributions of spectral effects are distinctly less important.

Fig. 2 and Fig. 3 outline the likeness between the slowest TOP-REX (Case 2) and the TOP-BAR in terms of power and reactivity, respectively: all the plotted curves arise from 2D-calculations. Due to the absence of significant spatial and spectral effects in Case 2, it follows that the TOP-BAR is well simulated also by the zerodimensional version of Case 2: and this occurs without a refined technique of simulating the control rod reactivity by "external reactivity". Anyway, no general conclusion is possible for two reasons at least. First, the results of

Fig. 2

CASES 2.4 - POWER VS TIME

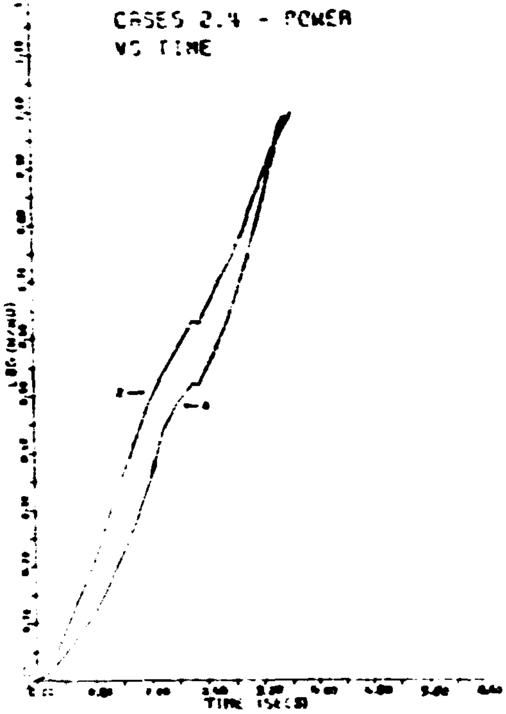

Fig. 3

CASES 2.4 REACTIVITY VS TIME

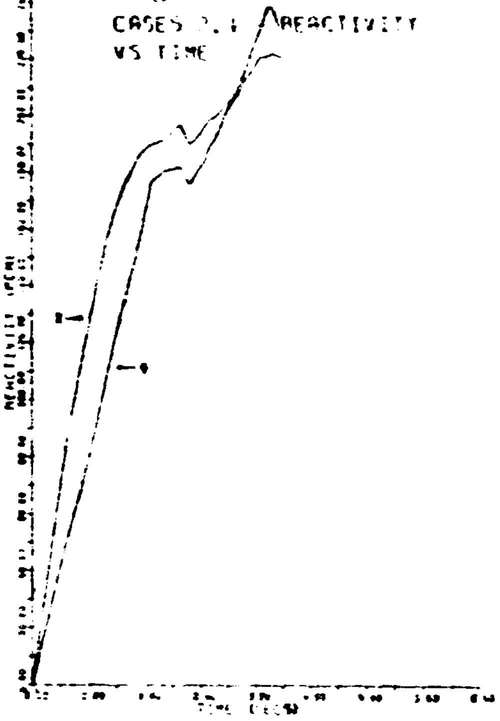

two cases tend to diverge in the final part of the transient: for example, the total reactivity increases at a rate of about 0.086 \$/sec in the TOP-BAR case and 0.164 \$/sec in the simulating calculation. Second, only the histories of integral parameters are well simulated: so, significant differences in the maximum fuel temperature occur and they can produce important divergences in the successive phase of accidents, after the fuel boiling.

In conclusion, only the rod accident, in the class of studied TOP accidents, suffers from shape effects, mostly due to spatial deformations. Very different is the situation in the field of LOF transients, where the shape effect is always important. Every transient can be divided into two well distinct phases:

a) the monophase transient, before the sodium boiling. The power and reactivity histories during this phase are shown in the second page of the annexed plots.

Due to the dominant contribution of the core deformation feedbacks, the reactivity is always negative, so that the power decreases with time. So, a positive Doppler reactivity is generated, which partially balances the deformation reactivity: this is particularly evident in the slow transient, where the energy dispersion from the fuel is significantly larger. Anyway, no important shape effects are evidenced. The maximum shape error occurs, in both cases, about 30 sec after the transient start and involves about -0.02 $. This error arises from a particular shape effect, the "epithermal effect", which consists on the spatial deformation of the epithermal neutron flux: its description is as followed. Due to the loss of flow, the sodium temperature increases with time, so that the heat flux from the fuel to the sodium tends to decrease, especially in the higher zones of the core. On the other hand, the decrease of power induces the cooling of the fuel. The former process is dominant in the higher zones, the latter in the lower ones: on the whole, the axial fuel temperature distribution is strongly modified, as shown in Fig.4 for the channel 4. Consequently, the inserted Doppler reactivity is negative in the upper zones, positive in the lower ones. This produces the axial deformation of the epithermal neutron flux, thus increasing the importance of the lower zones. Finally, a positive second order effect on the Doppler reactivity is generated. It is to be noted that the power distribution is practically unmodified, because the contribution of the epithermal neutrons to the total power is small.

The main consequence of the epithermal effect during this phase is the underevaluation of the power in the 0D-case and, consequently, the delay of the sodium boiling start, 32.5 sec in LOF-RIF and 0.5 sec in LOF-RAP.

b) the boiling transient. The main results of this phase are collected in the third page of the annexed plots. Clearly, the 0D-curves are shifted along the time axis to compensate for the delay of the boiling start. The qualitative reading of the LOF-RIF plots will be useful to outline the main characteristics of the performed calculations.

The sodium boiling starts in shell 4 above the upper blanket. The void reactivity appears to be near zero in the axial blankets and structures, negative in the higher and lower parts of the core, strongly positive in the central part. The voiding time is 0.4 sec on the whole. The reactivity of the first voiding is underestimated in the 0D calculation, due to the axially dishomogeneous void effect. In fact, in the 2D calculation, the neutron flux peak is accentuated by the fact that positive reactivity is added in the high-flux zones and subtracted in the low-flux ones. Consequently, the importance of the central zone is increased, and the void reactivity dishomogeneity is emphasized.

The spectral correction in the 0DC calculation produces a reduction not only of negative Doppler reactivity of the voiding phase, but also of the positive one generated during the monophase transient in shell 4. On

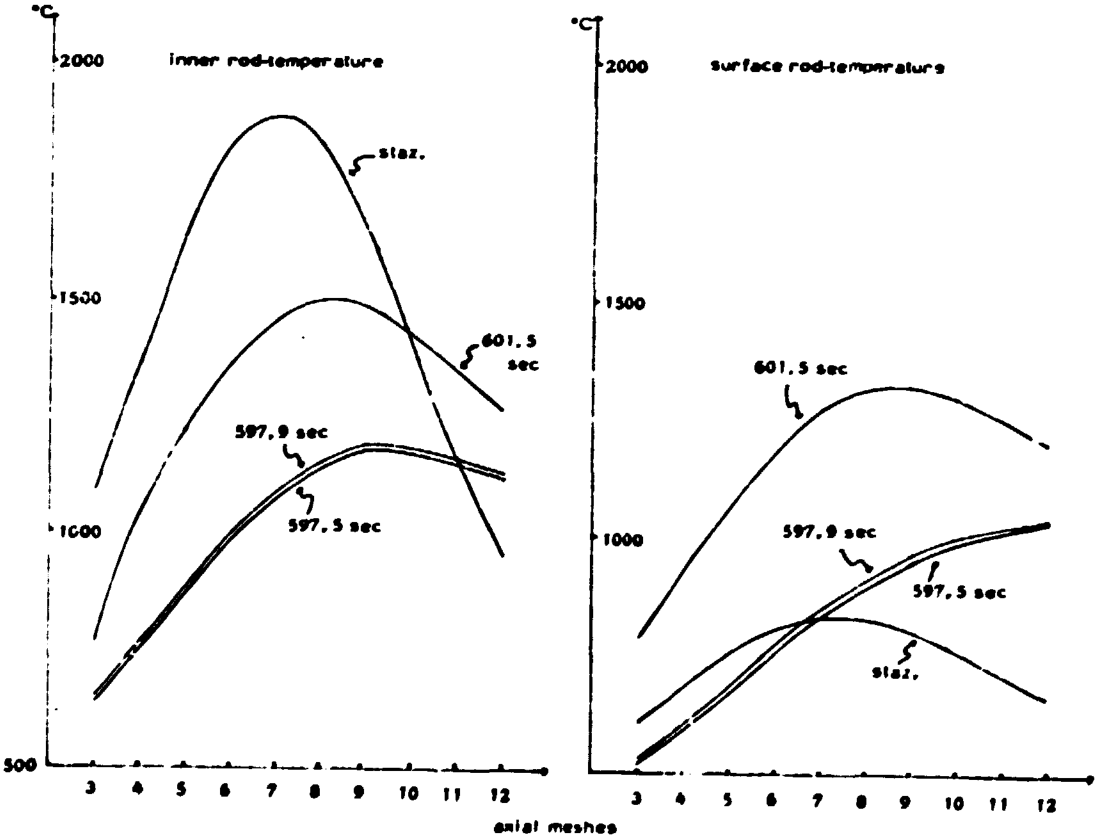

FIG. 4 : LOF-RIF - Axial temperature distribution in channel 4

the whole, the corrected reactivity contribution is in this case positive so that the reactivity underevaluation at the end of the first voiding is emphasized by the spectral correction.

The sodium reentry is not considered in the code, so that the decrease of the reactivity after the first voiding is mainly due to the Doppler effect. During this part of transient, about 3.5 sec long, the reactivity differences between the three versions of calculations tend to decrease, but the small persisting differences in the power levels are enough to strongly modify the boiling sequences. In particular, it is to be underlined that the reactivity superimposition due to the contemporaneous voiding of the channels 7 and 3 in the 2D case does not occur in the 0D cases.

A detailed analysis of the final part is not possible, due to the great number of interfering processes. However, it is not difficult to observe the effectiveness of the epithermal and spatial void effects, both in the axial and radial versions. From a qualitative point of view, the most important aspect of the shape effects in the final part is that the transients are ended by the feedbacks in the 0D cases, while the fuel melting and finally the fuel boiling occur in the 2D cases at a reactivity level of about 0.6 $. Moreover the spectral correction produces a major divergence between the 2D and 0D power histories and boiling sequences: it follows that the main spectral component of the shape effect and the spatial one have opposite signs. It is to be underlined that LOF-RIF and LOF-RAF results are coherent.

CONCLUSIONS AND PERSPECTIVES

The described results induce to conclude that very strong shape effects appear when any material relocation, including the sodium voiding, is involved in the transient. Detailed boiling sequences studies and systematic TOP-BAR analysis are needed to identify the possibility of simulating the material relocations by an "external reactivity"model. Finally, the shape effect during fuel relocation is to be studied. The general problem of defining the limits of the point kinetics now becomes the problem of constructing suitable simulation techniques in terms of "external reactivity".

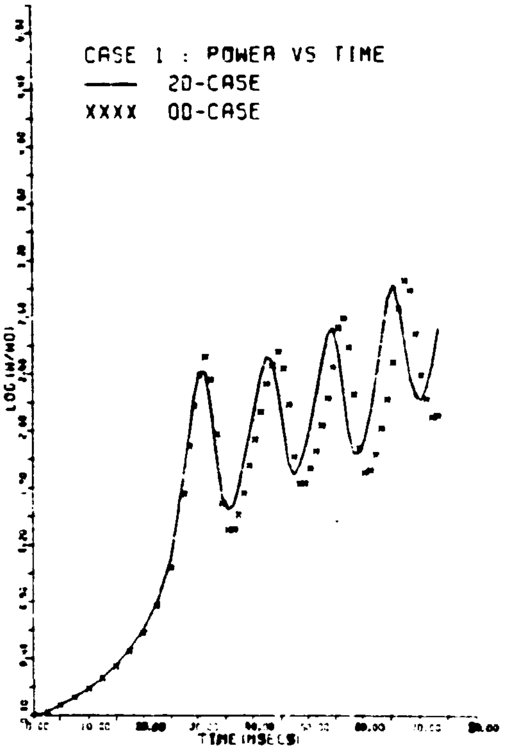
CASE 1 : POWER VS TIME
—— 2D-CASE
XXXX 0D-CASE
LOG(N/NO)
TIME(MSECS)

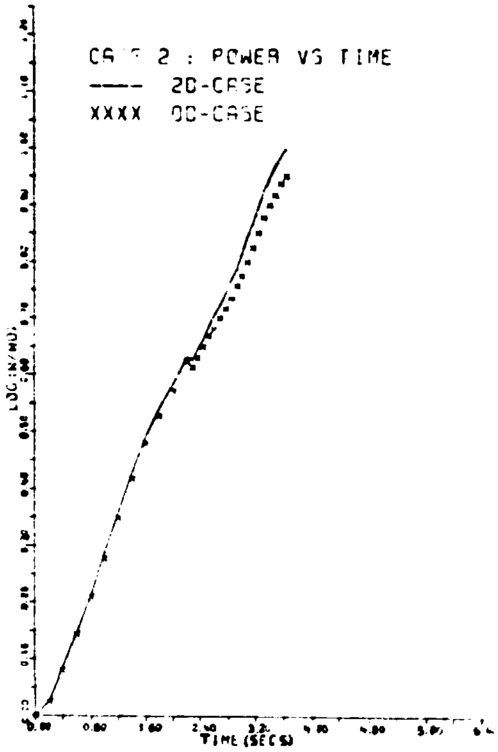
CASE 2 : POWER VS TIME
---- 2D-CASE
XXXX 0D-CASE
LOG(N/NO)
TIME(SECS)

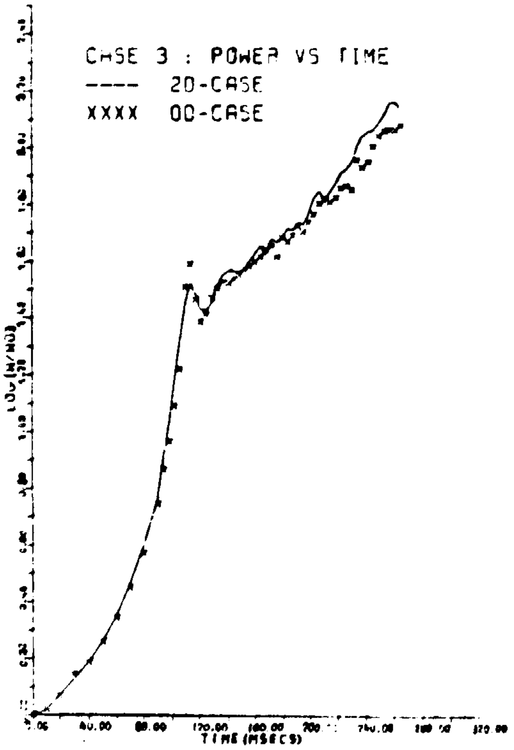
CASE 3 : POWER VS TIME
---- 2D-CASE
XXXX 0D-CASE
LOG(N/NO)
TIME(MSECS)

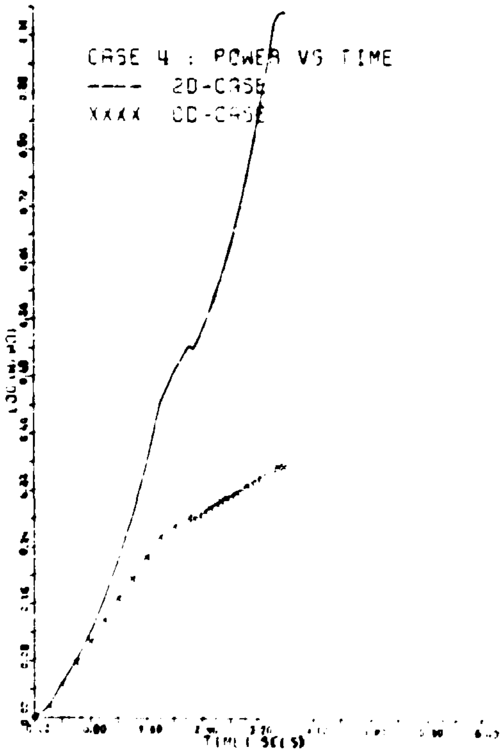
CASE 4 : POWER VS TIME
---- 2D-CASE
XXXX 0D-CASE
LOG(N/NO)
TIME(SECS)

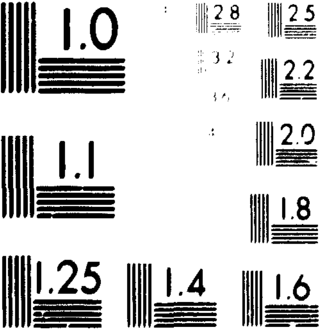
1.0
2.8
2.5
3.2
2.2
3.6
4
2.0
1.1
1.8
1.25
1.4
1.6

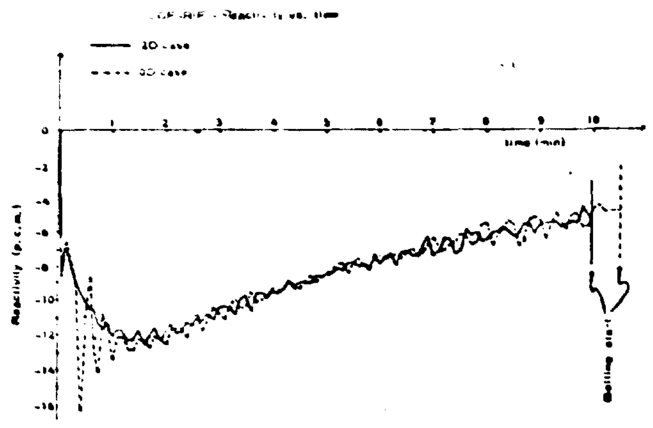
LOF-RIF - Reactivity vs. time
3D case
0D case
Reactivity (p.c.m.)
0
-2
-4
-6
-8
-10
-12
-14
-16
1
2
3
4
5
6
7
8
9
10
time (min)
Boiling start

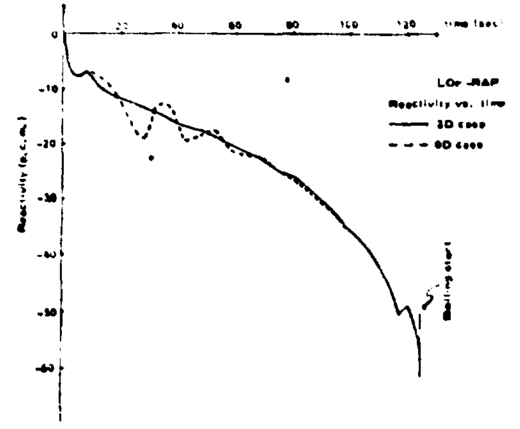
LOF-RAP
Reactivity vs. time
3D case
0D case
Reactivity (p.c.m.)
0
-10
-20
-30
-40
-50
-60
20
40
60
80
100
120
time (sec)
Boiling start

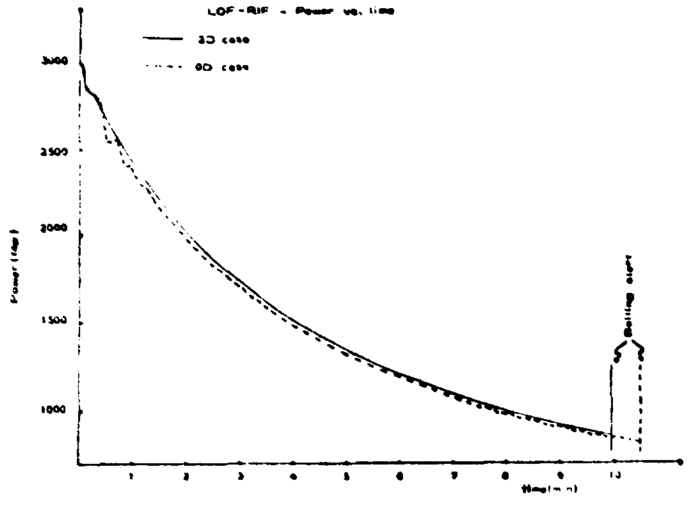
LOF-RIF - Power vs. time
3D case
0D case
Power (Mw)
3000
2500
2000
1500
1000
1
2
3
4
5
6
7
8
9
10
time (min)
Boiling start

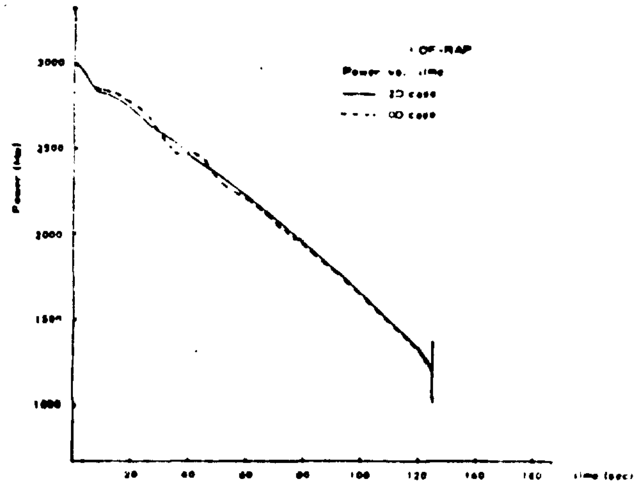
LOF-RAP
Power vs. time
3D case
0D case
Power (Mw)
3000
2500
2000
1500
1000
20
40
60
80
100
120
140
160
time (sec)

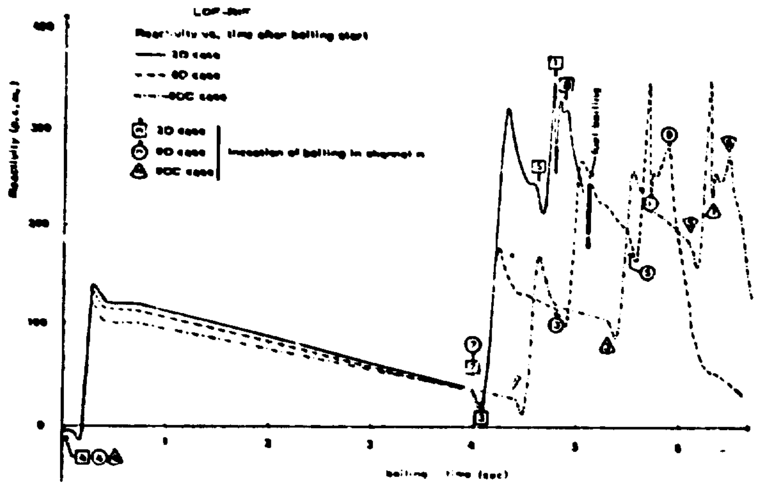
Reactivity vs. time after boiling start
—— 3D case
- - - 8D case
-·-·- 8DC case
3D case
8D case
8DC case
Inception of boiling in channel n
fuel boiling
Reactivity (¢)
0
100
200
300
400
boiling time (sec)
0
1
2
3
4
5
6

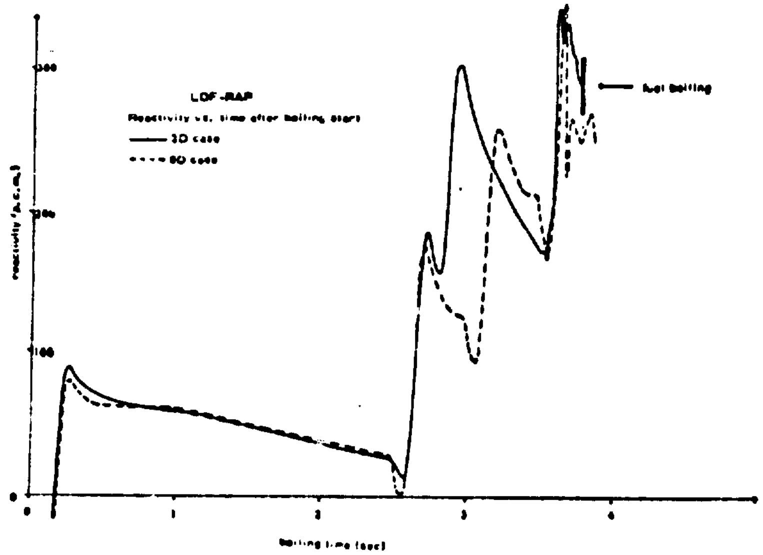
LOF-RAP
Reactivity vs. time after boiling start
—— 3D case
- - - 8D case
fuel boiling
Reactivity (¢)
0
100
200
300
Boiling time (sec)
0
1
2
3
4

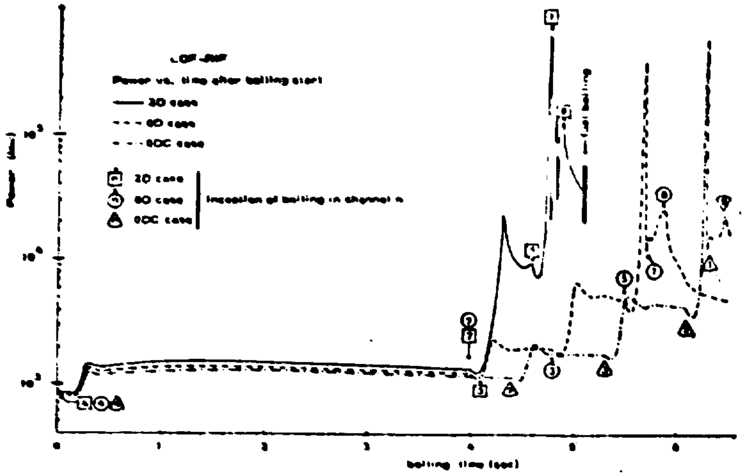
Power vs. time after boiling start
—— 3D case
- - - 8D case
-·-·- 8DC case
3D case
8D case
8DC case
Inception of boiling in channel n
fuel boiling
Power (Mw)
10^3
10^4
10^5
boiling time (sec)
0
1
2
3
4
5
6

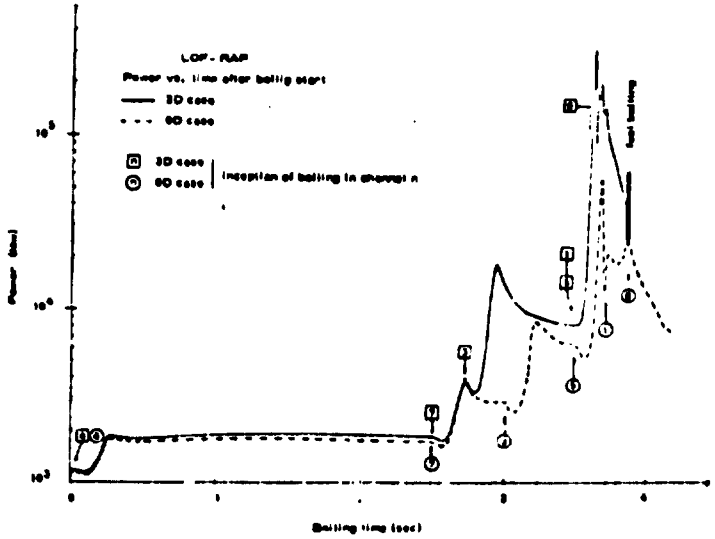
LOF-RAP
Power vs. time after boiling start
—— 3D case
- - - 8D case
3D case
8D case
Inception of boiling in channel n
fuel boiling
Power (Mw)
10^3
10^4
10^5
Boiling time (sec)
0
1
2
3
4

REFERENCES

/1/ G. BUFFONI, A. GALATI, R. MOSIELLO, A. MUSCO, F. NORELLI, C.D. STANESCU "NADYP, un codice di dinamica per reattori veloci: descrizione del modello fisico-matematico", RIT/FIS(74)8

/2/ A. GALATI, P. LOIZZO, A. MUSCO "Dinamica dei reattori veloci: 1) Messa a punto del codice NADYP", RT/FI(76)17

/3/ A. GALATI, A. MUSCO "Dinamica dei reattori veloci: 3) il codice NADYP-2", (in print)

/4/ A. GALATI "The metastatic method in nuclear reactor core kinetics calculation", N.S.E., 37(1969)

/5/ A. GALATI, P. LOIZZO, A. MUSCO "Dinamica dei reattori veloci: 4) effetti spaziali ed energetici nella fase di predisassemblaggio. Parte I: transitori di potenza", RIT/FIS-LTCR(78)2RR

/6/ A. GALATI "Dinamica dei reattori veloci: 4) effetti spaziali ed energetici nella fase di predisassemblaggio. Parte II: transitori di portata", RIT/FIS-LTCR(78)4RR